Immunity

Supplemental Information

The TREM2-APOE pathway drives the transcriptional phenotype of dysfunctional microglia in neurodegenerative diseases

Susanne Krasemann, Charlotte Madore, Ron Cialic, Caroline Baufeld, Narghes Calcagno, Rachid El Fatimy, Lien Beckers, Elaine O`Loughlin, Yang Xu, Zain Fanek, David J. Greco, Scott T. Smith, George Tweet, Zachary Humulock, Tobias Zrzavy, Patricia Conde-Sanroman, Mar Gacias, Zhiping Weng, Hao Chen, Emily Tjon, Fargol Mazaheri, Kristin Hartmann, Asaf Madi, Jason Ulrich, Markus Glatzel, Anna Worthmann, Joerg Heeren, Bogdan Budnik, Cynthia Lemere, Tsuneya Ikezu, Frank L. Heppner, Vladimir Litvak, David M. Holtzman, Hans Lassmann, Howard L. Weiner, Jordi Ochando, Christian Haass and Oleg Butovsky

Figure S1

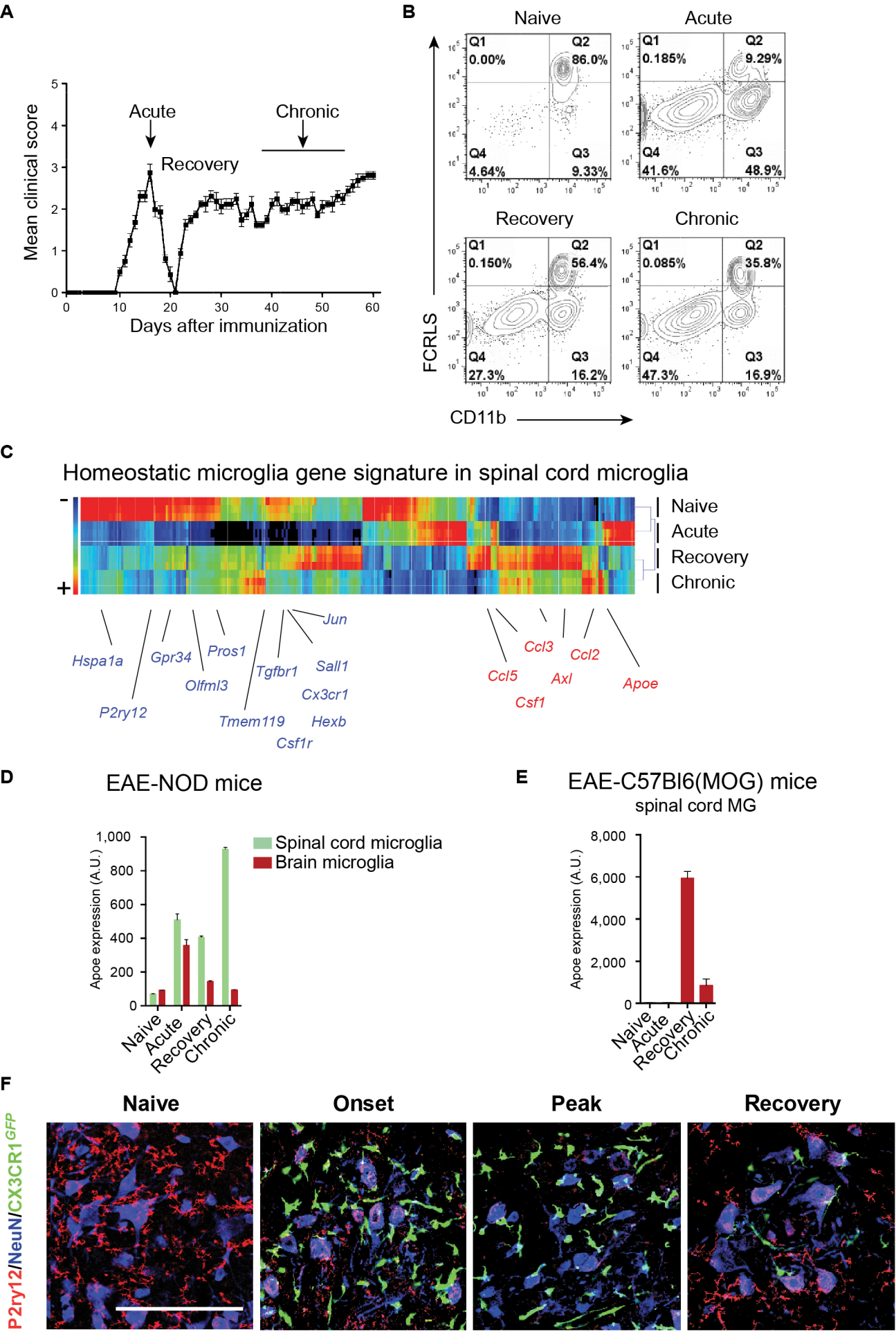
A
Mean clinical score
Acute
Chronic
Recovery
Days after immunization
B
Naive
Acute
Recovery
Chronic
Q1
Q2
Q3
Q4
0.00%
86.0%
4.64%
9.33%
0.185%
9.29%
41.6%
48.9%
0.150%
56.4%
27.3%
16.2%
0.085%
35.8%
47.3%
16.9%
FCRLS
CD11b
C
Homeostatic microglia gene signature in spinal cord microglia
Naive
Acute
Recovery
Chronic
Hspa1a
P2ry12
Gpr34
Olfml3
Pros1
Tmem119
Tgfbr1
Csf1r
Jun
Sall1
Cx3cr1
Hexb
Ccl5
Ccl3
Csf1
Axl
Ccl2
Apoe
D
EAE-NOD mice
Spinal cord microglia
Brain microglia
Apoe expression (A.U.)
Naive
Acute
Recovery
Chronic
E
EAE-C57Bl6(MOG) mice
spinal cord MG
Apoe expression (A.U.)
Naive
Acute
Recovery
Chronic
F
Naive
Onset
Peak
Recovery
P2ry12/NeuN/CX3CR1GFP

Figure S1. Microglia signature in EAE (related to Figure 1).
(A) Clinical scores of SJL-EAE mice are presented as mean ± s.e.m (n = 5). Spinal cords were collected at different disease stages during EAE.
(B) Representative FACS plots of FCRLS+CD11b+ microglia and gating strategy to isolate resident FCRLS+ microglia (Q2) from recruited myeloid cells (Q3).
(C) Heatmap of 275 significantly affected genes in FCRLS+ spinal cord microglia based on Nanostring expression profile in naïve and EAE mice at different disease stages; ANOVA, *$p < 0.05$. Each lane represents mean of pooled spinal cord microglia from naïve (n = 5) and SJL-EAE (n = 6) mice. Downregulated key homeostatic genes are highlighted in blue and upregulated inflammatory genes highlighted in red.
(D-E) qPCR analysis of Apoe expression in brain- and spinal cord-derived FCRLS+ microglia during disease stages in EAE-NOD (chronic) and (E) C57/Bl6 (acute) mouse models. Bars show relative expression of Apoe as compared to naïve microglia (n = 3 per disease stage). Expression levels were normalized to Gapdh. Data are presented as mean ± s.e.m. Shown is one of two individual experiments.
(F) Representative immunohistochemical staining for spinal cord sections at different disease stages in EAE Cx3cr1:GFP+/− chimera mice. Confocal immunofluorescent images of P2ry12+ resident microglia (red), NeuN+ neurons (blue), and Cx3Cr1-GFP (green) recruited myeloid cells in EAE chimeric mice at high magnification in the ventral horn. Scale bar, 200 μm. Each image represents similar results of 5 mice per group.
See also Table S1.

Figure S2

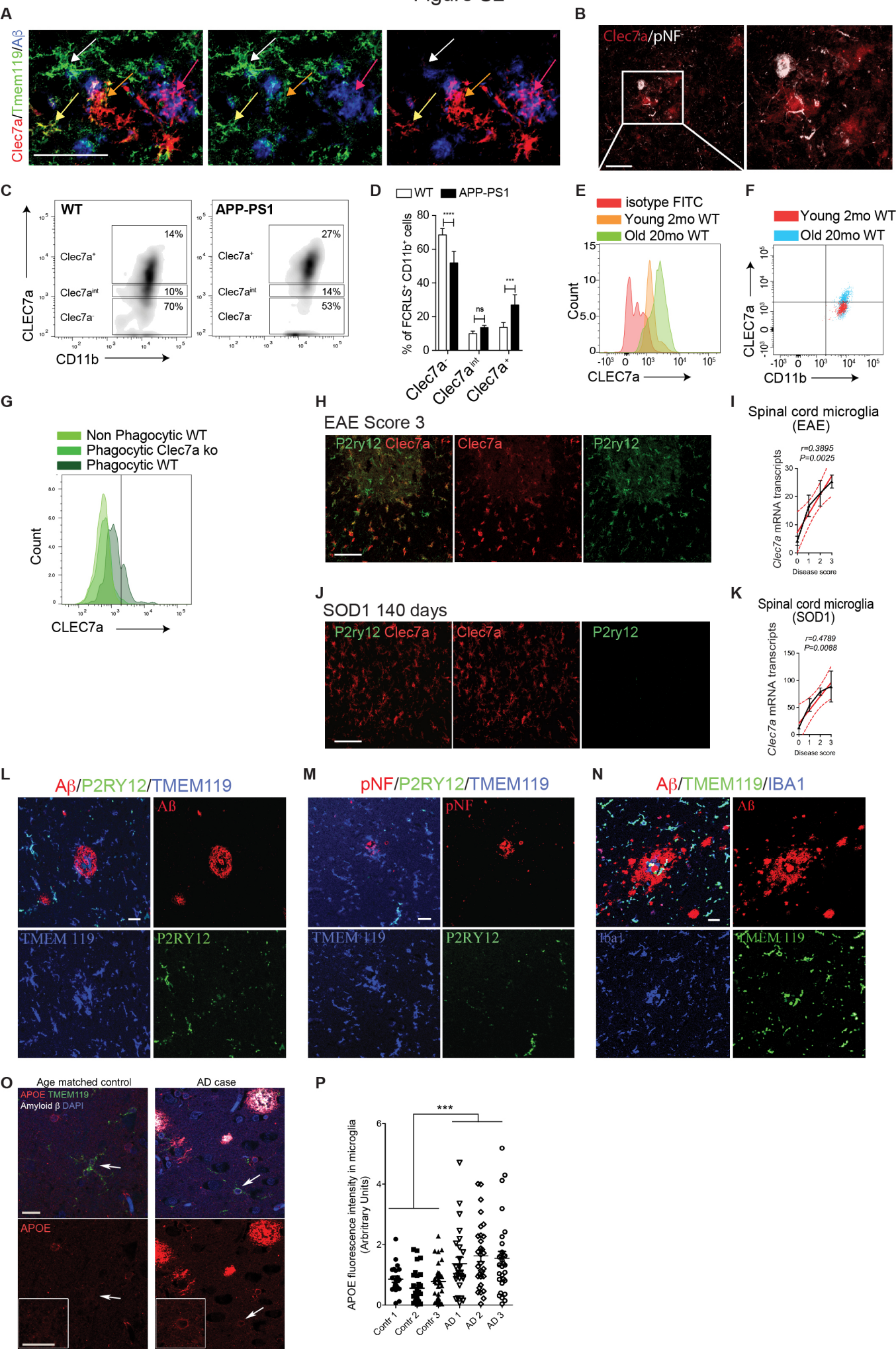
A
Clec7a/Tmem119/Aβ
B
Clec7a/pNF
C
WT
APP-PS1
14%
10%
70%
27%
14%
53%
Clec7a+
Clec7aint
Clec7a-
CLEC7a
CD11b
D
WT
APP-PS1
% of FCRLS+ CD11b+ cells
****
ns
***
Clec7a-
Clec7aint
Clec7a+
E
isotype FITC
Young 2mo WT
Old 20mo WT
Count
CLEC7a
F
Young 2mo WT
Old 20mo WT
CLEC7a
CD11b
G
Non Phagocytic WT
Phagocytic Clec7a ko
Phagocytic WT
Count
CLEC7a
H
EAE Score 3
P2ry12 Clec7a
Clec7a
P2ry12
I
Spinal cord microglia (EAE)
r=0.3895
P=0.0025
Clec7a mRNA transcripts
Disease score
J
SOD1 140 days
P2ry12 Clec7a
Clec7a
P2ry12
K
Spinal cord microglia (SOD1)
r=0.4789
P=0.0088
Clec7a mRNA transcripts
Disease score
L
Aβ/P2RY12/TMEM119
Aβ
TMEM 119
P2RY12
M
pNF/P2RY12/TMEM119
pNF
TMEM 119
P2RY12
N
Aβ/TMEM119/IBA1
Aβ
Iba1
TMEM 119
O
Age matched control
AD case
APOE TMEM119
Amyloid β DAPI
APOE
P
***
APOE fluorescence intensity in microglia (Arbitrary Units)
Contr 1
Contr 2
Contr 3
AD 1
AD 2
AD 3

Figure S2. Apoe and Clec7a are dysregulated in MGnD microglia in mice and humans (related to Figure 2).
(A) Representative immunohistochemical staining for TMEM119, Clec7a and Aβ in APP-PS1 mice (24-month-old). $Tmem119^{-}Clec7a^{+}$ microglia associated with Aβ plaque (red arrows). $Tmem119^{+}Clec7a^{+}$ microglia associated with Aβ plaque (orange arrows). $Tmem119^{+}Clec7a^{+}$ microglia and $Tmem119^{+}Clec7a^{-}$ microglia at close vicinity of the Aβ plaque (yellow and white arrows, respectively). Scale bar, 100 μm.
(B) Representative immunohistochemical staining of Clec7a and phosphorylated Neurofilament (pNF) in APP-PS1 mice (24-month-old). Scale bar, 20 μm.
(C) Representative FACS plots of $Clec7a^{+}$ vs. $Clec7a^{int}$ vs. $Clec7a^{-}$ $FCRLS^{+}$ microglia in APP-PS1 vs. WT mice (n = 5 per group; 24-month-old).
(D) Percentage of Clec7a cells in $FCRLS^{+}CD11b^{+}$ microglia in APP-PS1 vs. WT mice (n = 5 per group; 24-month-old). ***$p < 0.001$, Student t test, 2-tailed.
(E) Representative mean fluorescence intensity (MFI) of Clec7a and isotype control in young (2-month-old) and old (20-month-old) WT mice (n = 2 per group).
(F) Representative FACS plot of $Clec7a^{+}CD11b^{+}$ in young (2-month-old) and old (20-month-old) WT mice (n = 2 per group).
(G) Representative MFI of Clec7a in $FCRLS^{+}CD11b^{+}$ non-phagocytic and phagocytic microglia from WT and $Clec7a^{-/-}$ mice (n = 3 per group).
(H) Representative immunohistochemical staining of P2ry12 and Clec7a in spinal cord at the peak of EAE (score = 3). Scale bar, 100 μm.
(I) Linear regression curve of Clec7a expression in spinal cord microglia from EAE with different disease scores. Thick line indicates 95% confidence interval of the regression line.
(J) Representative immunohistochemical staining of P2ry12 and Clec7a in spinal cord of SOD1 mice at 140 days (endstage). Scale bar, 100 μm.
(K) Linear regression curve of Clec7a expression in spinal cord microglia in SOD1 mice at different disease scores. Thick line indicates 95% confidence interval of the regression line.
(L) Representative immunohistochemical analysis of human AD brain for TMEM119 (blue), P2RY12 (green) and Aβ plaque (red). Scale bar, 20 μm.
(M) Representative immunohistochemical analysis of human AD brain for TMEM119 (blue), P2RY12 (green) and pNF (red) for neuritic plaque. Scale bar, 20 μm.
(N) Representative immunohistochemical analysis of human AD brain for TMEM119 (green), IBA1 (blue) and Aβ (red) for Aβ plaque. Scale bar, 20 μm.
(O) Representative immunohistochemical analysis of human AD brain and an age-matched control for APOE (red), Aβ (white), DAPI (blue) and TMEM119 (green). White arrows indicate $TMEM119^{+}$ microglia and co-expression of APOE in AD case. Scale bar, 20 μm.
(P) Quantification of APOE fluorescence intensity in $TMEM119^{+}$ microglia in AD and age-matched controls (n = 3 per group). Data points represent staining intensity of APOE per individual cell in 300 μm^2, (A.U. arbitrary units). ***$p < 0.005$ (one-way ANOVA). Of note, cells close to amyloid-plaques or astrocytes were excluded due to potential overlap in APOE-content.
See also Table S1.

Figure S3

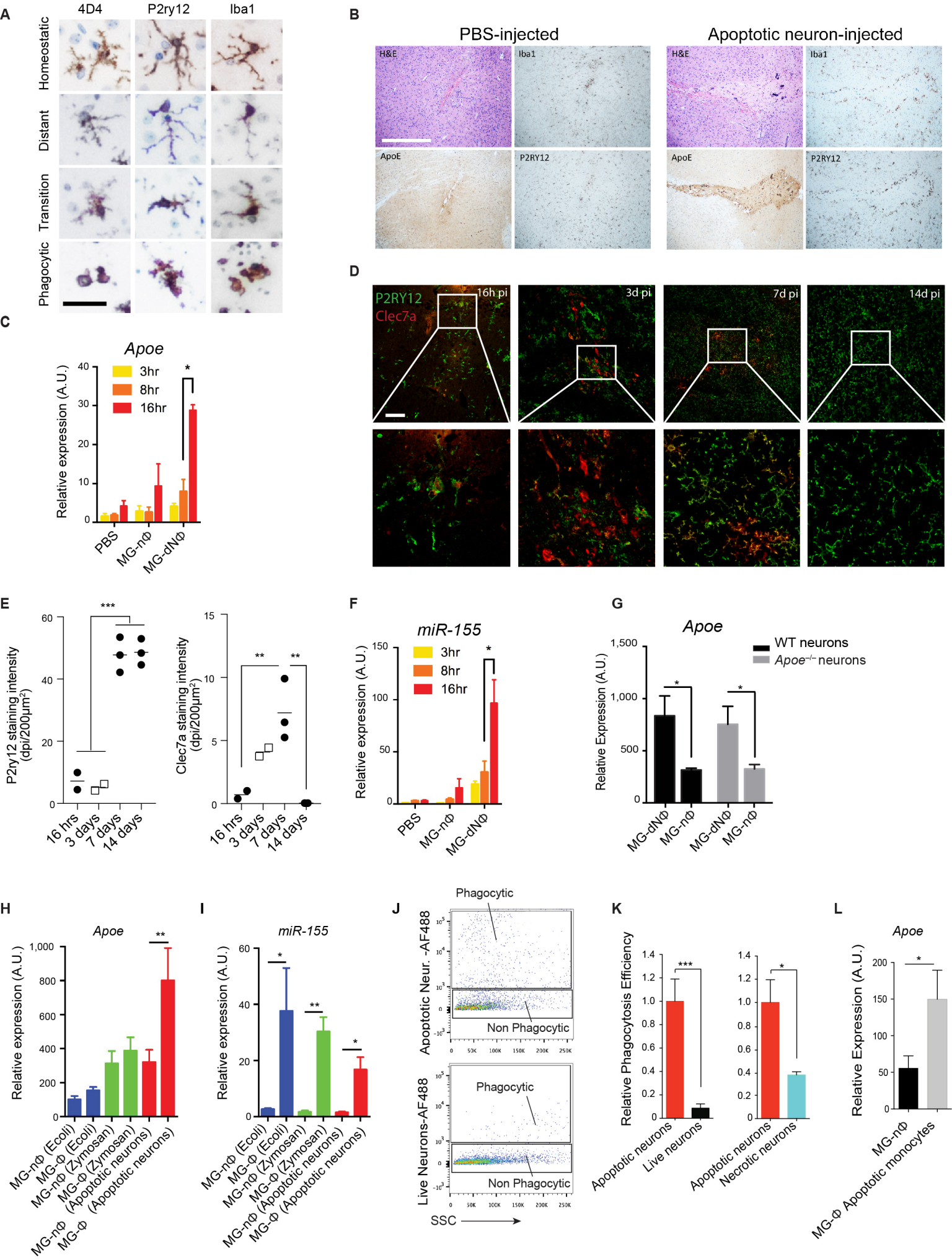
A
4D4
P2ry12
Iba1
Homeostatic
Distant
Transition
Phagocytic
B
PBS-injected
Apoptotic neuron-injected
H&E
Iba1
ApoE
P2RY12
C
Apoe
3hr
8hr
16hr
Relative expression (A.U.)
PBS
MG-nΦ
MG-dNΦ
D
P2RY12
Clec7a
16h pi
3d pi
7d pi
14d pi
E
P2ry12 staining intensity (dpi/200μm²)
Clec7a staining intensity (dpi/200μm²)
16 hrs
3 days
7 days
14 days
F
miR-155
Relative expression (A.U.)
G
Apoe
WT neurons
Apoe−/− neurons
Relative Expression (A.U.)
H
Apoe
Relative expression (A.U.)
MG-nΦ (Ecoli)
MG-Φ (Ecoli)
MG-nΦ (Zymosan)
MG-Φ (Zymosan)
MG-nΦ (Apoptotic neurons)
MG-Φ (Apoptotic neurons)
MG-nΦ
MG-Φ
I
miR-155
Relative expression (A.U.)
J
Phagocytic
Apoptotic Neur. -AF488
Non Phagocytic
Live Neurons-AF488
SSC
K
Relative Phagocytosis Efficiency
Apoptotic neurons
Live neurons
Necrotic neurons
L
Apoe
Relative Expression (A.U.)
MG-nΦ
MG-Φ Apoptotic monocytes

Figure S3. Apoptotic neurons affect microglia phenotype and specifically induce *Apoe* expression in phagocytic microglia (related to Figure 3).

(A) Representative close-up pictures of homeostatic microglia, microglia distant from the injection site, microglia in transition and amoeboid phenotype stained with microglial specific antibodies P2ry12 and 4D4 or macrophage/microglia marker Iba1, 16 h post-injection of apoptotic neurons. Scale bar, 5 µm.

(B) Representative immunohistochemical analysis of mouse brains injected with PBS (n = 5) or apoptotic neurons (n = 5) 16 h post-injection stained for hematoxylin-eosin (H&E), Iba1, Apoe and P2ry12. Scale bar, 250 µm.

C) qPCR analysis of *Apoe* gene expression in $FCRLS^+$ MG-dNΦ vs. MG-nΦ microglia. $Alexa488^+$ apoptotic neurons were stereotaxically injected in WT mice and $FCRLS^+$ microglia were sorted at 3, 8 or 16 h post-injection. PBS injection served as control. *Apoe* expression level was normalized against *Gapdh* using ΔCt (n = 3, per group). Data are presented as mean normalized expression ± s.e.m. *p < 0.05 (one-way ANOVA followed by Tukey's multiple-comparison *post hoc* test).

(D) Representative immunohistochemical staining for P2ry12 and Clec7a at 16 h, 3, 7 and 14 d post-injection of apoptotic neurons. Scale bar, 100 µm. Area in white boxes is magnified in lower panel. Scale bar, 50 µm.

(E) Quantification of P2ry12 and Clec7a fluorescence intensity at 16 h, 3, 7 and 14 d post-injection of apoptotic neurons. Data points represent staining intensity (dpi) per 200 μm^2, **p<0.01, ***p < 0.001 (one-way ANOVA).

(F) miR-155 expression in $FCRLS^+$ MG-dNΦ vs. MG-nΦ microglia. $Alexa488^+$ apoptotic neurons were stereotaxically injected in WT mice and $FCRLS^+$ microglia were sorted at 3, 8 or 16 h post-injection. PBS injection served as control. miR-155 expression was normalized against U6 miRNA using ΔCt (n = 3 per group). Data are presented as mean normalized expression ± s.e.m. *p < 0.05 (one-way ANOVA followed by Tukey's multiple-comparison *post hoc* test).

(G) qPCR analysis of $FCRLS^+$ MG-dNΦ vs. MG-nΦ microglia sorted from mouse brains 16 h post-injection with apoptotic neurons derived from WT or $Apoe^{-/-}$ mice (n = 3 per group). Expression levels were normalized to *Gapdh* using ΔCt (n = 3 per group). Data are presented as mean ± s.e.m. *p < 0.05, Student's t test, 2-tailed. Shown is one of two individual experiments.

(H-I) qPCR analysis of *Apoe* gene expression (H) and miR-155 expression (I) in $FCRLS^+$ MG-dNΦ vs. MG-nΦ microglia after injection of $Alexa488^+$ apoptotic neurons, *E.coli* and Zymosan particles 16 h post-injection. *Apoe* expression was normalized against *Gapdh* and miR-155 expression was normalized against U6 miRNA using ΔCt (n = 3 per group). Data are presented as mean normalized expression ± s.e.m. *p < 0.05, **p < 0.01 (one-way ANOVA followed by Tukey's multiple-comparison *post hoc* test). Shown is one of two individual experiments.

(J) Representative FACS-plots of $FCRLS^+$ microglia phagocyting $Alexa488^+$ apoptotic vs. live neurons, 16 h post-injection.

(K) Quantification of phagocytosis efficiency of apoptotic vs. live neurons and necrotic neurons (n = 5 per group). Bars show relative fold change (mean ± s.e.m) (*p < 0.05, ***p < 0.001 by Student t test, 2-tailed).

(L) qPCR analysis of *Apoe* gene expression in $FCRLS^+$ MG-dNΦ containing $Alexa488^+$ apoptotic monocytes and MG-nΦ, 16 h post-injection. Gene expression level was normalized against *Gapdh* using ΔCt (n = 5, per group). Data are presented as mean normalized expression ± s.e.m. *p < 0.05, Student's t test, 2-tailed.

Figure S4

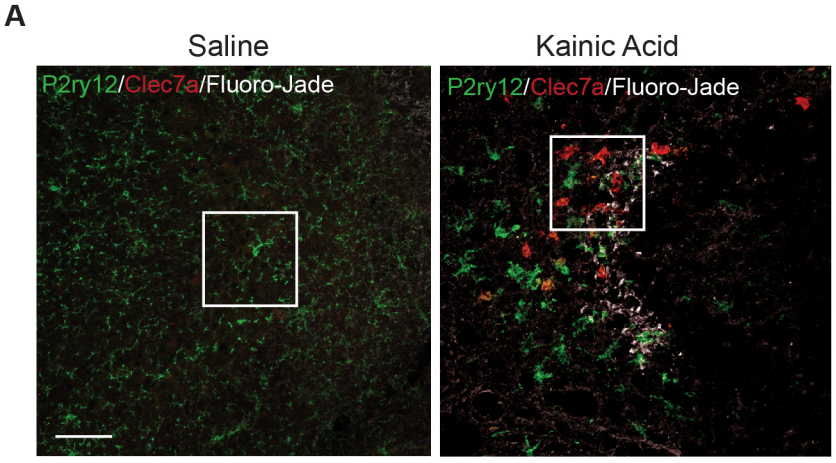
A
Saline
Kainic Acid
P2ry12/Clec7a/Fluoro-Jade
P2ry12/Clec7a/Fluoro-Jade

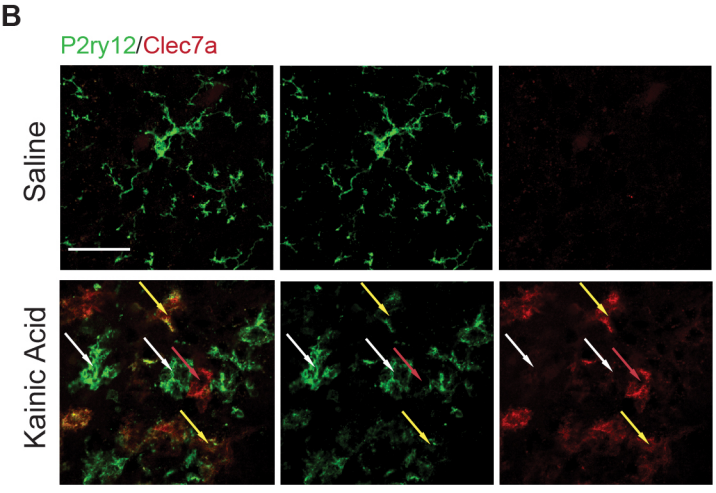
B
P2ry12/Clec7a
Saline
Kainic Acid

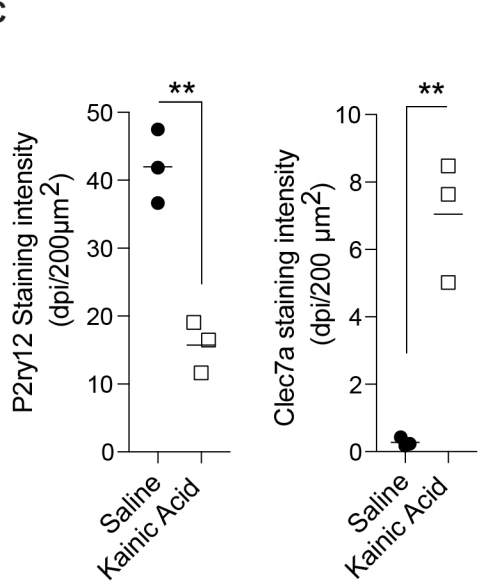
C
**
P2ry12 Staining intensity (dpi/200µm2)
50
40
30
20
10
0
Saline
Kainic Acid
**
Clec7a staining intensity (dpi/200 µm2)
10
8
6
4
2
0
Saline
Kainic Acid

Figure S4. Intrahippocampal injection of Kainic acid induces MGnD microglia (related to Figure 3).
(A) Representative immunohistochemical staining for P2ry12, Clec7a and Fluoro-Jade (degenerating neurons) in the CA3 region of saline and kainic acid injected hippocampi. Scale bar, 100 μm.
(B) High magnifications of immunohistochemical staining for P2ry12 and Clec7a in the CA3 region of saline and kainic acid injected hippocampi shown in white boxes (A). Scale bar, 50 μm. White arrows point to homeostatic $P2ry12^{+}Clec7a^{-}$ microglia, yellow arrows point to transitioning $P2ry12^{+}Clec7a^{+}$ microglia, red arrow points to MGnD $P2ry12^{-}Clec7a^{+}$ microglia. Scale bar, 50 μm.
(C) Quantifications of P2ry12 and Clec7a staining intensity in the CA3 region of saline and kainic acid injected hippocampi (n = 3 per treatment). Data points represent staining intensity (dpi) per 200 μm^2, **$p < 0.01$ by Student t test, 2-tailed.

Figure S5

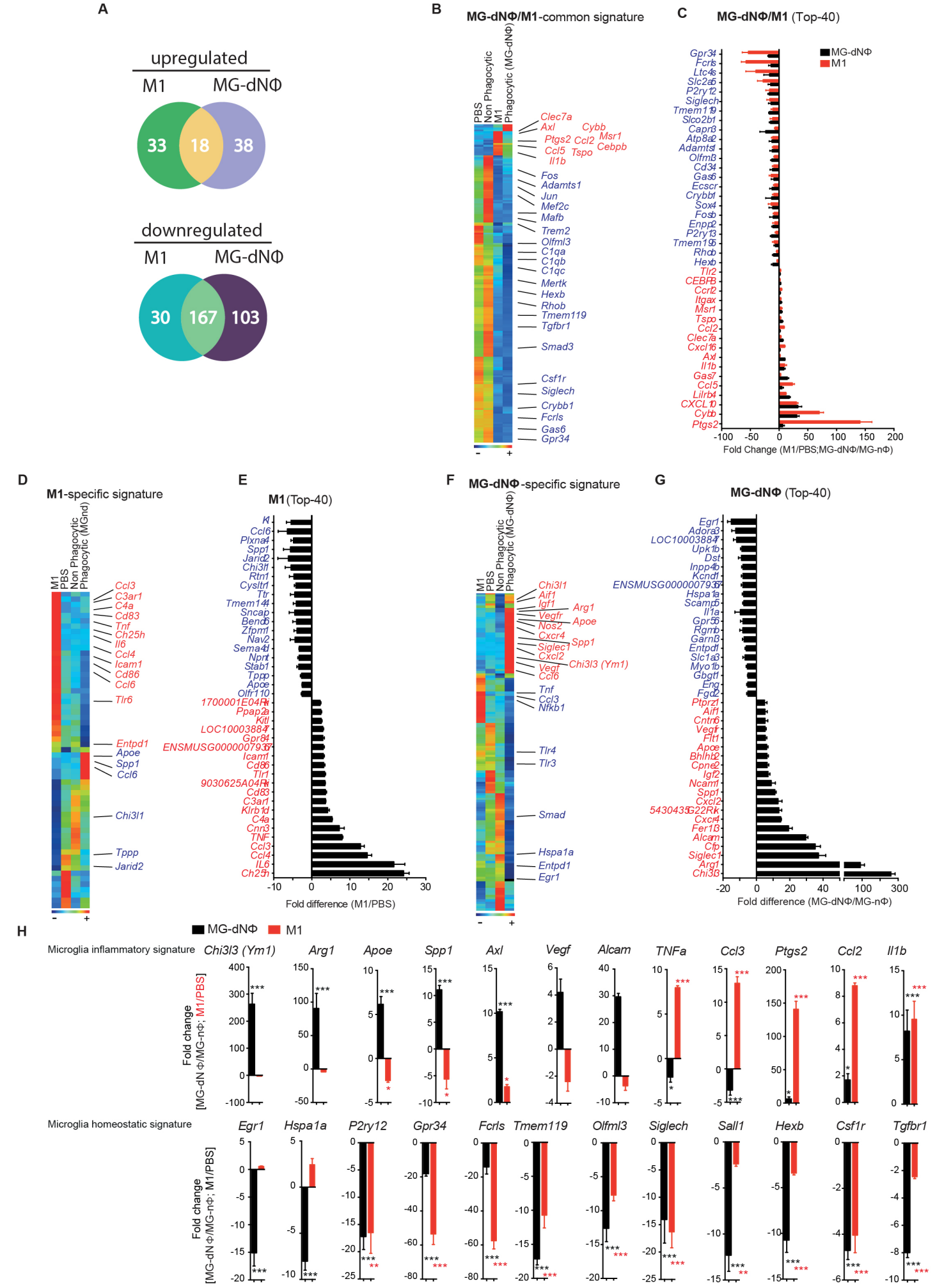
A
upregulated
M1
MG-dNΦ
33
18
38
downregulated
M1
MG-dNΦ
30
167
103
B
MG-dNΦ/M1-common signature
PBS
Non Phagocytic
M1
Phagocytic (MG-dNΦ)
Clec7a
Axl
Cybb
Ptgs2
Ccl2
Msr1
Ccl5
Tspo
Cebpb
Il1b
Fos
Adamts1
Jun
Mef2c
Mafb
Trem2
Olfml3
C1qa
C1qb
C1qc
Mertk
Hexb
Rhob
Tmem119
Tgfbr1
Smad3
Csf1r
Siglech
Crybb1
Fcrls
Gas6
Gpr34
C
MG-dNΦ/M1 (Top-40)
MG-dNΦ
M1
Gpr34
Fcrls
Ltc4s
Slc2a5
P2ry12
Siglech
Tmem119
Slco2b1
Capn3
Atp8a2
Adamts1
Olfml3
Cd34
Gas6
Ecscr
Crybb1
Sox4
Fosb
Enpp2
P2ry13
Tmem125
Rhob
Hexb
Tlr2
CEBPB
Ccrl2
Itgax
Msr1
Tspo
Ccl2
Clec7a
Cxcl16
Axl
Il1b
Gas7
Ccl5
Lilrb4
CXCL10
Cybb
Ptgs2
-100
-50
0
50
100
150
200
Fold Change (M1/PBS;MG-dNΦ/MG-nΦ)
D
M1-specific signature
M1
PBS
Non Phagocytic
Phagocytic (MGnd)
Ccl3
C3ar1
C4a
Cd83
Tnf
Ch25h
Il6
Ccl4
Icam1
Cd86
Ccl6
Tlr6
Entpd1
Apoe
Spp1
Ccl6
Chi3l1
Tppp
Jarid2
E
M1 (Top-40)
Kl
Ccl6
Plxna4
Spp1
Jarid2
Chi3l1
Rtn1
Cysltr1
Ttr
Tmem144
Sncap
Bend5
Zfpm1
Nav2
Sema4d
Npnt
Stab1
Tppp
Apoe
Olfr110
1700001E04Rik
Ppapdc2a
Kitl
LOC100038847
Gpr84
ENSMUSG00000079357
Icam1
Cd86
Tlr1
9030625A04Rik
Cd83
C3ar1
Klrb1d
C4a
Cnr3
TNF
Ccl3
Ccl4
IL6
Ch25h
-10
0
10
20
30
Fold difference (M1/PBS)
F
MG-dNΦ-specific signature
M1
PBS
Non Phagocytic
Phagocytic (MG-dNΦ)
Chi3l1
Aif1
Igf1
Arg1
Vegfr
Apoe
Nos2
Cxcr4
Spp1
Siglec1
Cxcl2
Chi3l3 (Ym1)
Vegf
Ccl6
Tnf
Ccl3
Nfkb1
Tlr4
Tlr3
Smad
Hspa1a
Entpd1
Egr1
G
MG-dNΦ (Top-40)
Egr1
Adora3
LOC100038847
Upk1b
Dst
Inpp4b
Kcnd1
ENSMUSG00000079357
Hspa1a
Scamp5
Il1a
Gpr56
Rgmb
Garnl3
Entpd1
Slc1a3
Myo1b
Gbgt1
Eng
Fgd2
Ptprz1
Aif1
Cntn6
Vegf
Flt1
Apoe
Bhlhb2
Cpne2
Igf2
Ncam1
Spp1
Cxcl2
5430435G22Rik
Cxcr4
Fer1l3
Alcam
Cfp
Siglec1
Arg1
Chi3l3
-20
0
20
40
100
300
Fold difference (MG-dNΦ/MG-nΦ)
H
MG-dNΦ
M1
Microglia inflammatory signature
Chi3l3 (Ym1)
Arg1
Apoe
Spp1
Axl
Vegf
Alcam
TNFa
Ccl3
Ptgs2
Ccl2
Il1b
Fold change [MG-dN Φ/MG-nΦ; M1/PBS]
Microglia homeostatic signature
Egr1
Hspa1a
P2ry12
Gpr34
Fcrls
Tmem119
Olfml3
Siglech
Sall1
Hexb
Csf1r
Tgfbr1
Fold change [MG-dN Φ/MG-nΦ; M1/PBS]

Figure S5. Molecular comparison of MG-dNΦ vs. M1 microglia (related to Figure 3). Gene expression profiles of FCRLS^{+} microglia sorted 16 h post-injection from LPS- and IFNγ- (100 ng and 10ng per injection site, respectively) (n = 18) vs. PBS-injected brains (n = 15) (see Table S4 for complete dataset), were compared to gene expression profiles of MG-dNΦ phagocytic microglia (n = 4) vs. non-phagocytic (n = 4).
(A) Venn diagram shows common and unique up- and down-regulated genes in M1 vs. MG-dNΦ microglia.
(B) Heatmap of MG-dNΦ/M1-common signature.
(C) Top-40 up- and down-regulated genes in the common MG-dNΦ and M1signature.
(D) Heatmap of M1-specific signature.
(E) Top-40 up- and down-regulated genes specific to M1 signature.
(F) Heatmap of MG-dNΦ specific signature.
(G) Top-40 up- and down-regulated genes specific to MG-dNΦ signature.
(H) Expression of key genes between M1 and MG-dNΦ microglia. Bars show mRNA counts per 100 ng total RNA as mean ± s.e.m. *$p < 0.05$, **$p < 0.01$, ***$p < 0.001$, Student's t test, 2-tailed.
See also Table S3.

Figure S6

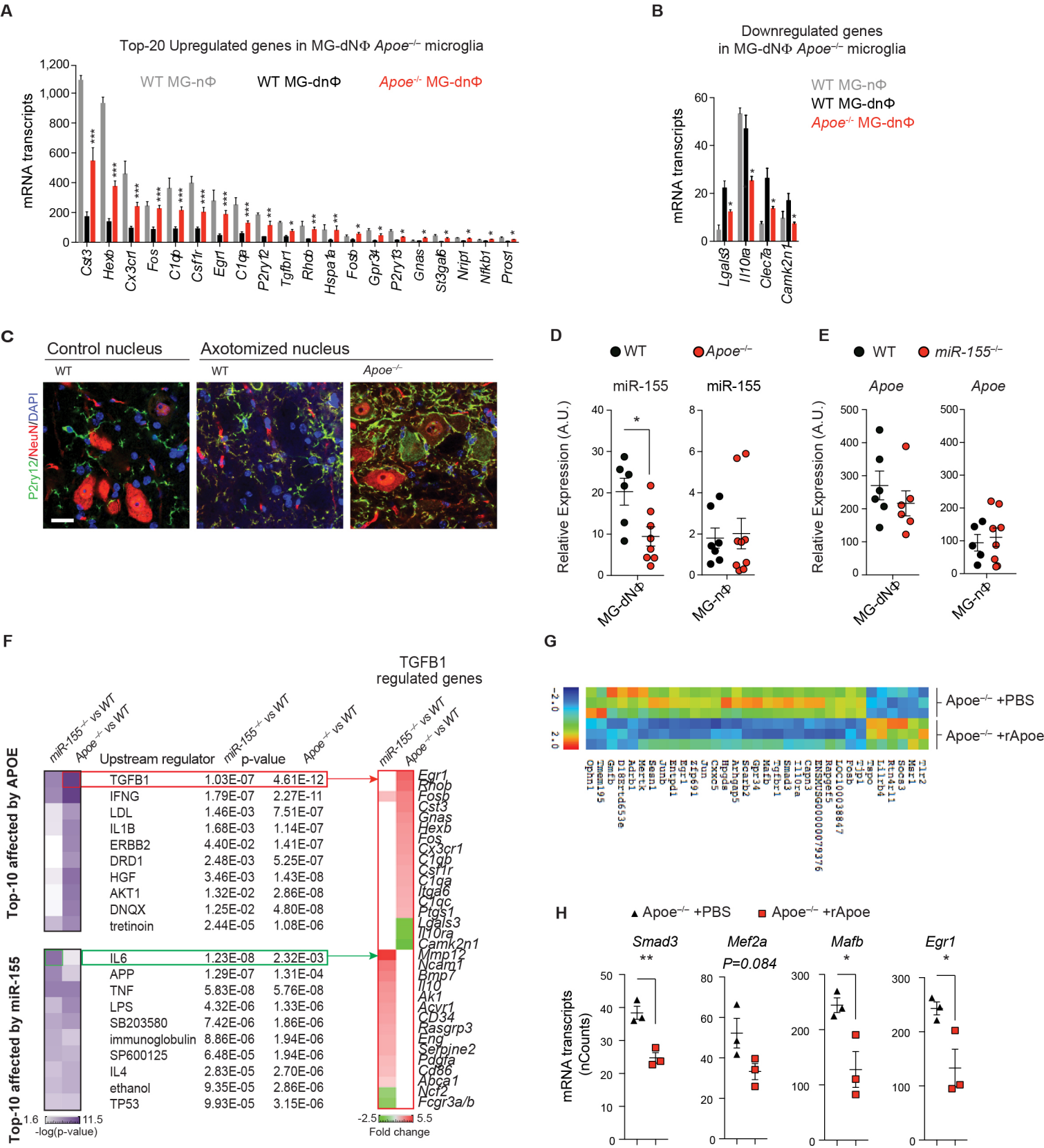
A
Top-20 Upregulated genes in MG-dNΦ Apoe-/- microglia
WT MG-nΦ
WT MG-dnΦ
Apoe-/- MG-dnΦ
mRNA transcripts
Cst3
Hexb
Cx3cr1
Fos
C1qb
Csf1r
Egr1
C1qa
P2ry12
Tgfbr1
Rhob
Hspa1a
Fosb
Gpr34
P2ry13
Gnas
St3gal6
Nrip1
Nfkb1
Prosl
B
Downregulated genes
in MG-dNΦ Apoe-/- microglia
WT MG-nΦ
WT MG-dnΦ
Apoe-/- MG-dnΦ
mRNA transcripts
Lgals3
Il10ra
Clec7a
Camk2n1
C
Control nucleus
Axotomized nucleus
WT
WT
Apoe-/-
P2ry12/NeuN/DAPI
D
WT
Apoe-/-
miR-155
miR-155
Relative Expression (A.U.)
MG-dNΦ
MG-nΦ
E
WT
miR-155-/-
Apoe
Apoe
Relative Expression (A.U.)
MG-dNΦ
MG-nΦ
F
TGFB1
regulated genes
miR-155-/- vs WT
Apoe-/- vs WT
Upstream regulator
p-value
miR-155-/- vs WT
Apoe-/- vs WT
Top-10 affected by APOE
TGFB1 1.03E-07 4.61E-12
IFNG 1.79E-07 2.27E-11
LDL 1.46E-03 7.51E-07
IL1B 1.68E-03 1.14E-07
ERBB2 4.40E-02 1.41E-07
DRD1 2.48E-03 5.25E-07
HGF 3.46E-03 1.43E-08
AKT1 1.32E-02 2.86E-08
DNQX 1.25E-02 4.80E-08
tretinoin 2.44E-05 1.08E-06
Top-10 affected by miR-155
IL6 1.23E-08 2.32E-03
APP 1.29E-07 1.31E-04
TNF 5.83E-08 5.76E-08
LPS 4.32E-06 1.33E-06
SB203580 7.42E-06 1.86E-06
immunoglobulin 8.86E-06 1.94E-06
SP600125 6.48E-05 1.94E-06
IL4 2.83E-05 2.70E-06
ethanol 9.35E-05 2.86E-06
TP53 9.93E-05 3.15E-06
Egr1
Rhob
Fosb
Cst3
Gnas
Hexb
Fos
Cx3cr1
C1qb
Csf1r
C1qa
Itga6
C1qc
Ptgs1
Lgals3
Il10ra
Camk2n1
Mmp12
Ncam1
Bmp7
Il10
Ak1
Acvr1
CD34
Rasgrp3
Eng
Serpine2
Pdgfa
Cd86
Abca1
Ncf2
Fcgr3a/b
1.6
11.5
-log(p-value)
-2.5
5.5
Fold change
G
Apoe-/- +PBS
Apoe-/- +rApoe
H
Apoe-/- +PBS
Apoe-/- +rApoe
Smad3
Mef2a
P=0.084
Mafb
Egr1
mRNA transcripts
(nCounts)

Figure S6. Targeting APOE signaling restores homeostatic microglia (related to Figure 4).
(A-B) Nanostring expression profile of (A) top-20 significantly upregulated and (B) downregulated genes in FACS-sorted FCRLS^{+} MG-dNΦ microglia from WT and *Apoe*$^{-/-}$ brains injected with Alexa488^{+} apoptotic neurons as compared to MG-nΦ microglia from the same injection site (n = 3 per group). Bars show mRNAs transcripts (mean ± s.e.m) per 100 ng of total RNA. *p < 0.05, **p < 0.01, ***p < 0.001 (one-way ANOVA followed by Tukey's multiple-comparison *post hoc* test). Data represent one of two independent experiments.
(C) High magnification of representative immunohistochemical staining for NeuN^{+} and P2ry12^{+} in contralateral vs. axotomized facial motor nucleus 7 d post-surgery in WT vs. *Apoe*$^{-/-}$ mice (n = 5 per group). Scale bar, 20 μm.
(D) qPCR analysis of miR-155 expression in MG-nΦ vs. MG-dNΦ microglia from WT vs. *Apoe*$^{-/-}$ mice (n = 6-8 per group). Gene expression level was normalized for miR-155 expression against U6 miRNA using ΔCt. Data are presented as mean normalized expression ± s.e.m. *p < 0.05, by Student t test, 2-tailed.
(E) qPCR analysis of *Apoe* expression in MG-nΦ vs. MG-dNΦ microglia from WT vs. *miR-155*$^{-/-}$ mice (n = 6-8 per group). Gene expression level was normalized for *Apoe* expression against *Gapdh* using ΔCt. Data are presented as mean normalized expression ± s.e.m. *p < 0.05, by Student t test, 2-tailed.
(F) IPA pathway analysis shows top-10 most significantly affected upstream regulators in the expression profiles of FCRLS^{+} phagocytic microglia from *Apoe*$^{-/-}$ vs. miR-155$^{-/-}$ mice (n = 6-8 per group). Of note, TGFβ is the most derepressed gene in phagocytic microglia from *Apoe*$^{-/-}$ mice. Data are presented as mean ± s.e.m. *p < 0.05, **p < 0.01, ***p < 0.001 by one-way ANOVA followed by Tukey´s multiple-comparison *post-hoc* test.
(G) Heatmap of significantly affected genes, 16 h post-injection, in FCRLS^{+} FACS-sorted microglia from *Apoe*$^{-/-}$ mice injected with recombinant Apoe (rApoe) or PBS (control) as determined by nCounter (n = 3 per group).
(H) Selected genes shown in (G). Dot plots show mRNAs transcripts (mean ± s.e.m). *p<0.05, **p<0.01, ***p<0.001, ****p< 0.0001 by one-way ANOVA followed by Tukey´s multiple-comparison *post-hoc* test.
See also Table S5.

Figure S7

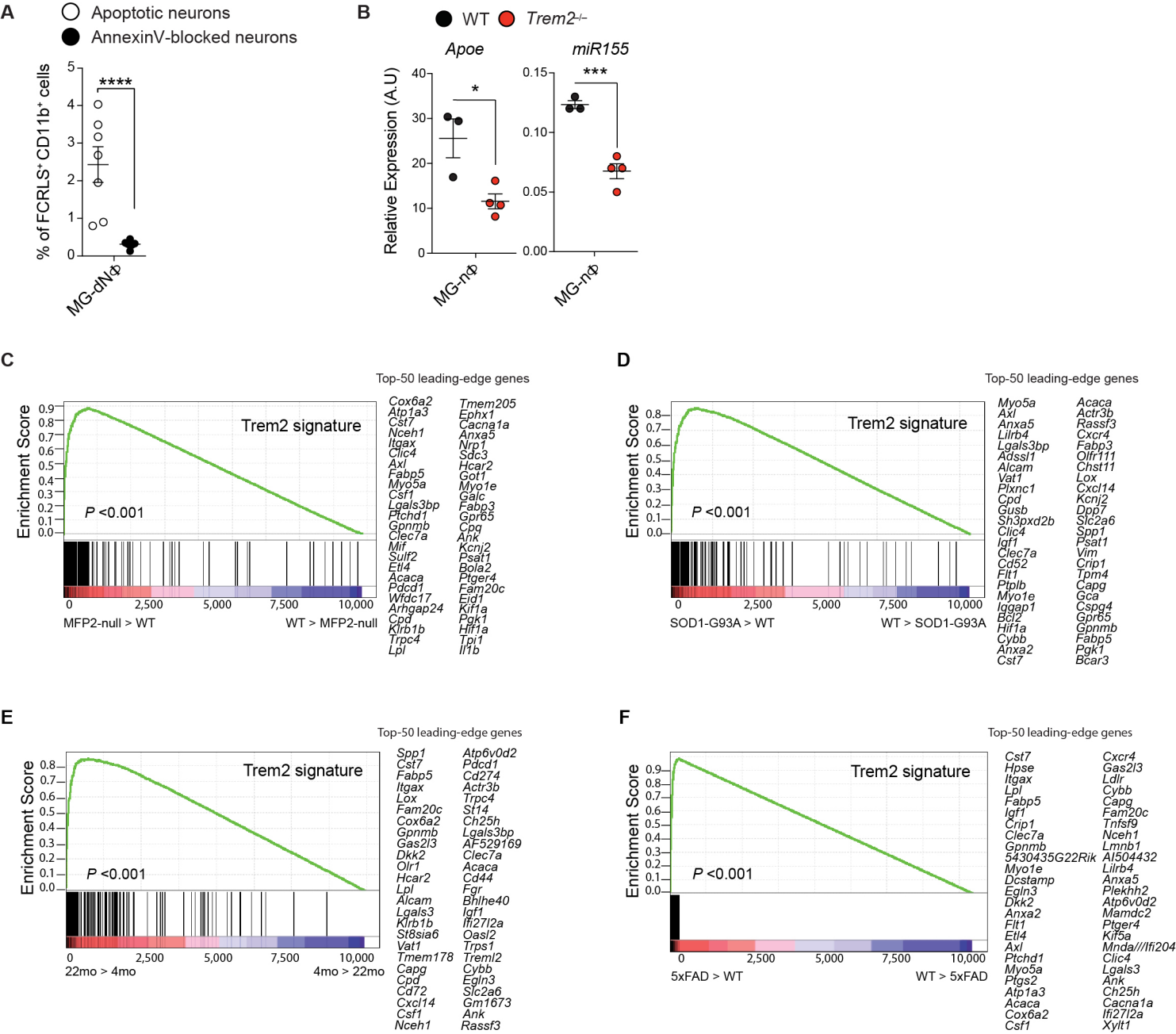
A
Apoptotic neurons
AnnexinV-blocked neurons
% of FCRLS+ CD11b+ cells
****
MG-dNΦ
B
WT
Trem2-/-
Apoe
miR155
Relative Expression (A.U)
*
***
MG-nΦ
MG-nΦ
C
Top-50 leading-edge genes
Trem2 signature
Enrichment Score
P <0.001
MFP2-null > WT
WT > MFP2-null
Cox6a2 Atp1a3 Cst7 Nceh1 Itgax Clic4 Axl Fabp5 Myo5a Csf1 Lgals3bp Ptchd1 Gpnmb Clec7a Mif Sulf2 Eif4 Acaca Pdcd1 Wfdc17 Arhgap24 Cpd Klrb1b Trpc4 Lpl
Tmem205 Ephx1 Cacna1a Anxa5 Nrp1 Sdc3 Hcar2 Got1 Myo1e Galc Fabp3 Gpr65 Cpq Ank Kcnj2 Psat1 Bola2 Ptger4 Fam20c Eid1 Kif1a Pgk1 Hif1a Tpi1 Il1b
D
Top-50 leading-edge genes
Trem2 signature
Enrichment Score
P <0.001
SOD1-G93A > WT
WT > SOD1-G93A
Myo5a Axl Anxa5 Lilrb4 Lgals3bp Adssl1 Alcam Vat1 Plxnc1 Cpd Gusb Sh3pxd2b Clic4 Igf1 Clec7a Cd52 Flt1 Ptplb Myo1e Iggap1 Bcl2 Hif1a Cybb Anxa2 Cst7
Acaca Actr3b Rassf3 Cxcr4 Fabp3 Olfr111 Chst11 Lox Cxcl14 Kcnj2 Dpp7 Slc2a6 Spp1 Psat1 Vim Crip1 Tpm4 Capg Gca Cspg4 Gpr65 Gpnmb Fabp5 Pgk1 Bcar3
E
Top-50 leading-edge genes
Trem2 signature
Enrichment Score
P <0.001
22mo > 4mo
4mo > 22mo
Spp1 Cst7 Fabp5 Itgax Lox Fam20c Cox6a2 Gpnmb Gas2l3 Dkk2 Olr1 Hcar2 Lpl Alcam Lgals3 Klrb1b St8sia6 Vat1 Tmem178 Capg Cpd Cd72 Cxcl14 Csf1 Nceh1
Atp6v0d2 Pdcd1 Cd274 Actr3b Trpc4 St14 Ch25h Lgals3bp AF529169 Clec7a Acaca Cd44 Fgr Bhlhe40 Igf1 Ifi27l2a Oasl2 Trps1 Treml2 Cybb Egln3 Slc2a6 Gm1673 Ank Rassf3
F
Top-50 leading-edge genes
Trem2 signature
Enrichment Score
P <0.001
5xFAD > WT
WT > 5xFAD
Cst7 Hpse Itgax Lpl Fabp5 Igf1 Crip1 Clec7a Gpnmb 5430435G22Rik Myo1e Dcstamp Egln3 Dkk2 Anxa2 Flt1 Etl4 Axl Ptchd1 Myo5a Ptgs2 Atp1a3 Acaca Cox6a2 Csf1
Cxcr4 Gas2l3 Ldlr Cybb Capg Fam20c Tnfsf9 Nceh1 Lmnb1 AI504432 Lilrb4 Anxa5 Plekhh2 Atp6v0d2 Mamdc2 Ptger4 Kif5a Mnda///Ifi204 Clic4 Lgals3 Ank Ch25h Cacna1a Ifi27l2a Xylt1

Figure S7. TREM2 implication in microglia regulation in disease (related to Figure 5).
(A) Quantification of phagocytosis efficiency of apoptotic vs. Annexin V-pretreated apoptotic neurons (n = 5 per group). Data are presented as mean ± s.e.m. ****p < 0.001 by Student t test, 2-tailed.
(B) qPCR analysis of *Apoe* and miR-155 expression in non-phagocytic (MG-nΦ) microglia from Trem2$^{-/-}$ vs. WT mice (n = 3-4 per group). Data are presented as mean ± s.e.m normalized against *Gapdh* and U6 expression using ΔCt. *p < 0.05, by Student t test, 2-tailed.
(C-F), GSEA plots demonstrate the over-representation of TREM2 signature (derived from GSE65067) in APP-PS1, *Mfp2*$^{-/-}$, SOD1 and Aging microglia transcriptomes of (C) *Mfp2*$^{-/-}$ mice; (D) aged mice; (E) SOD1 mice; and (F) 5xFAD mice compared with WT microglia. Genes are ranked into an ordered list according to their differential expression. The middle part of the plot is a bar code demonstrating the distribution of genes in the TREM2 transcriptional signature gene set against the ranked list of genes. The list on the right shows the top genes in the leading-edge subset.
See also Table S6.

TREM2 Genotype	APOE Genotype	Age	Gender	Braak Stage	Estimated CDR
WT	E3/E3	96	Female	Stage VI	3
WT	E3/E3	81	Male	Stage VI	3
R62H	E3/E4	89	Female	Stage VI	3
R47H	E3/E4	78	Male	Stage V	3
WT	E4/E4	72	Male	N/A	n/A
R47H	E4/E4	75	Male	Stage V	2
WT	E4/E4	72	Male	Stage VI	3
R62H	E3/E4	78	Male	N/A	N/A
WT	E3/E4	80	Male	N/A	N/A
R62H	E4/E4	83	Female	N/A	3
WT	E3/E4	85	Female	N/A	3

Table S7. Human AD subjects carrying AD-associated *TREM2* variants (related to Figure 6). Cortex samples from AD patients with and without mutations in TREM2 were sampled and characterized at the University of Washington (St. Louis). Demographic and Clinical Features including age, gender and disease severity (Braak stage, estimated CDR), and *APOE* and *TREM2* genotype was determined for each patient.